INCLUSION REMOVAL BY CAO-SIO_2-AL_2O_3-MGO SLAGS IN EXPERIMENTAL CONDITIONS*

Vinicius Cardoso da Rocha[1]
Pedro Cunha Alves[2]
Julio Aníbal Morales Pereira[3]
Augusto Lachini Pereira[4]
Wagner Viana Bielefeldt[5]
Antônio Cezar Faria Vilela[6]

Abstract
The capacity of steelmaking slags (CaO-SiO_2-Al_2O_3-MgO) on inclusion removal from liquid steel was investigated through experimental conditions. Laboratory experiments with slag and steel samples (with inclusion population known) were performed using a vertical electric resistance furnace at 1600 ºC. After the melting experiments, slag and steel samples were separated and analyzed regarding their chemical composition and inclusion population evolution. The capacity of slags on inclusion removal was evaluated based on the thermodynamics (solid and liquid phases proportion, phase composition and effective viscosity of slags) calculated using the *FactSage*™ 7.2. Results indicated that changes in the composition of slags (regarding CaO/SiO_2 e Al_2O_3) presented effects on the steel cleanliness. The total inclusion density decreased in all steel samples and the removal of inclusions by slags shows a tendency to improve as their viscosity decreases (< 0.23 Pa.s).
Keywords: Inclusion removal; Steelmaking slags; Computational thermodynamics; FactSage

[1] *Metallurgical Engineering, MSc, Dr. student, Iron and Steelmaking Lab. (LaSid), Federal University of Rio Grande do Sul, Porto Alegre, Rio Grande do Sul, Brasil.*
[2] *Metallurgical Engineering, MSc, researcher, Iron and Steelmaking Lab. (LaSid), Federal University of Rio Grande do Sul, Porto Alegre, Rio Grande do Sul, Brasil.*
[3] *Metallurgical Engineering, Dr., researcher, Iron and Steelmaking Lab. (LaSid), Federal University of Rio Grande do Sul, Porto Alegre, Rio Grande do Sul, Brasil.*
[4] *Metallurgical Engineering Undergraduate, scientific initiation scholarship, Iron and Steelmaking Lab. (LaSid), Federal University of Rio Grande do Sul, Porto Alegre, Rio Grande do Sul, Brasil.*
[5] *Metallurgical Engineering, Dr., professor, Iron and Steelmaking Lab. (LaSid), Federal University of Rio Grande do Sul, Porto Alegre, Rio Grande do Sul, Brasil.*
[6] *Metallurgical Engineering, Dr.-Ing, titular professor, Iron and Steelmaking Lab. (LaSid), Federal University of Rio Grande do Sul, Porto Alegre, Rio Grande do Sul, Brasil.*

** Technical contribution to the 50º Seminário de Aciaria, part of the ABM Week 2019, October 1st-3rd, 2019, São Paulo, SP, Brazil.*

1 INTRODUCTION

The secondary steelmaking process adopts $CaO\text{-}SiO_2$ based slags to promote the refining of the liquid steel. Among these slags, the $CaO\text{-}SiO_2\text{-}Al_2O_3\text{-}MgO$ (CSAM) system is one of the most common and disseminated, where CaO, SiO_2, Al_2O_3 and MgO levels exceed 90% in mass of all other (minority) compounds. The optimization of the chemical composition of these slags is pursued, in order to have modifications in its physical properties and, consequently, providing better refining conditions of the liquid steel.

The phrase "look after the slag and the metal will look after itself" [1] represents well the idea of relation between slags with the melt. The interpretation of this phrase makes it possible to understand the important role of slag in the liquid steel refining. In others words, well design slags will tend to produce good quality steels. Regarding the inclusionary cleanliness, the control of the chemical composition of the slag will reflect in the population of inclusions present in the steel, both from the point of view of the chemical composition of these inclusions as well as their amount.

Using specific technological equipment it is possible to study the effect of secondary steelmaking slags on the inclusion removal. The automatic analysis allows to identify and classify the inclusions present in a certain steel sample area, making possible the evaluation of the density and area fraction of inclusions per steel sample. In addition, the use of computational thermodynamics tools allows to establish relevant effects involving the phase distribution, viscosity and also saturation of the slags applied for the steel production. It is important to note that viscosity is one of the most important physical properties of slag. According to Jiang, Wang and Wang [2] a change in the composition of slag may also result in a change in viscosity which affects the ability of slag to remove inclusions. Strandh *et al*. [3] reinforce that slag viscosity is a critical parameter to define the effective removal of an inclusion so that it overcomes the interface barrier between slag and steel and does not return to the liquid metal. Therefore, the joint analysis of all these information, promoted by several robust analysis techniques, allows a very rich evaluation of the slag in the performance of its inclusionary cleanliness function.

Within the context described, the main objective of this study is to present the capacity of different slags of the CSAM system in the removal of inclusions by using experimental and thermodynamic methodologies. With respect to the specific objectives, it is highlighted the consolidation of a methodology for the study of slag in steel cleanliness, thermodynamic calculations of slag (phase fraction, MgO saturation, viscosity) and the relationships with the analysis of inclusions.

2 MATERIALS AND METHODS

2.1 Experimental approach

Four samples of steel and slag with 100 and 20 g/each, respectively, were melted in a vertical resistive electric furnace (Figure 1) at 1600 ºC and held at that temperature for 90 minutes. The melting process were carried out in MgO-C crucibles (with internal diameter = 32 mm and height = 100 mm) containing the steel and slag samples, under Argon gas (99.999% pure, with N_2 < 3 ppm and O_2 < 1 ppm) with a constant flowing atmosphere of 82 l/h. All four crucibles were placed in a support (C-based) for the melting process in a single experiment. This practice was adopted in

previous studies [4,5] and can reduce experimental costs, increase productivity and provide exactly the same experimental conditions for all samples.

The steel samples were collected after the rolling process, being cut and properly prepared for the experiment. The slags were a mixture of pure reagent grade CaO, Al_2O_3, SiO_2, MgO. The chemical compositions of the slags were measured by X-ray fluorescence (XRF) technique using *Philips* equipment (model PW2600) and the steel samples by optical emission spectrometer (model ARL-4460). Specifically for the analysis of total oxygen (T.O.) and nitrogen in steel samples, the LECO TC-400 equipment was applied. Tables 1 and 2 present the initial chemical composition of steel and slag samples, respectively. It is important to mention that the steel has a low Ca content (around 2 ppm), and therefore was not considered in the present study.

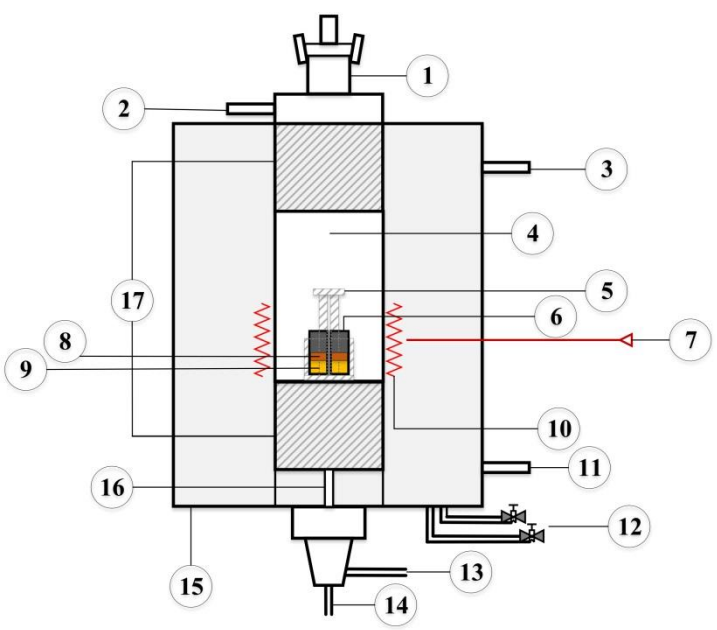

(1) Furnace access door
(2) Gas inlet tube
(3) Gas inlet chamber
(4) Graphite tube
(5) Crucible support (C-based)
(6) Crucible
(7) Furnace thermocouple
(8) Slag sample
(9) Steel sample
(10) Heating element
(11) Gas outlet chamber
(12) Inlet/outlet water (for cooling)
(13) Vacuum pump
(14) Gas filter
(15) Stainless steel housing
(16) Gas outlet tube
(17) Thermal insulation system

Figure 1. Vertical resistive electric furnace.

Table 1. Initial chemical composition of steel, wt.%.

C	Si	Mn	P	Cr	Ni	Mo	Al	Ca*	S*	T.O.*	N*
0.60	0.23	0.84	0.021	0.16	0.04	0.01	0.019	2	90	23.3	106.6

**ppm; T.O.: total oxygen;*

Table 2. Initial chemical composition of slags, wt.%.

Sample	CaO	SiO_2	Al_2O_3	MgO	wt. % CaO/ wt. % SiO_2	wt.% CaO/ wt.% Al_2O_3
1	48	32	10	10	1.5	4.80
2	57.5	22.5	10	10	2.5	5.75
3	42	28	20	10	1.5	2.10
4	50	20	20	10	2.5	2.50

For the inclusion analysis, an ASPEX Explorer equipment was applied, with an acceleration voltage of 20 kV and distance focus of 17 mm. The analyzed areas of steel samples range from 138.4 to 185 mm^2. Based on the analysis of these areas, it is possible to obtain information such as density (number of inclusions per sample area) and area fraction of all inclusions identified (as proposed by Equation 1).

$$Area\ fraction = \sum inclusions\ area\ [mm^2]/sample\ area\ [mm^2] \quad (1)$$

The ASPEX Explorer equipment has a scanning electron microscope (SEM) with an energy-dispersive spectrometer (EDS) and provides an automated elementary analysis of the chemical elements present within inclusions. The results of elementary analysis were converted into stable oxides (CaO, SiO_2, Al_2O_3 and MgO) through stoichiometric relationships of the compound in question, the atomic mass of the element, and the mass measured in the EDS analysis. This conversion was obtained with the support of an *MS Excel* spreadsheet developed at the Ironmaking and Steelmaking Laboratory (LaSid/UFRGS). It should be noted that in this study only the inclusions identified and classified by ASPEX were considered.
The population of inclusions in the steel samples was also determined before the experiments (in the initial steel sample). This analysis becomes very relevant for the study of slag capacity in the removal of inclusions, due to the possibility to identify the variation of the inclusion population caused by the effect of the refining slag. Thus, taking into account the difference in the density of inclusions between the initial and final steel samples (after experiment), the removal capacity was performed. The removal efficiency was calculated through the module of this difference and divided by the initial condition. Conveniently, the result is analyzed as a percentage.

2.2 Thermodynamic approach

The capacity of slags on inclusion removal was evaluated also based on the thermodynamics using *FactSage*™ 7.2. The modules used in the software were the *Equilib* (to obtain the solid/liquid fractions of the slag and its chemical compositions in equilibrium) and *Viscosity* (for viscosity calculation of liquid slags). In the *Equilib* module, the databases used were two: *FactPS* (for stoichiometric pure substances) and *FToxid* (for oxides and sulfur). The *Viscosity* module uses *Melts* databases and provides the liquid viscosity (η) that was applied in the model proposed by Roscoe-Einstein [6], according to Equation 2.

$$\eta_e = \eta\,(1 - c)^{-2.5} \quad (2)$$

The Equation 2 is used to calculate the effective viscosity of slags (η_e), considering the effect of the solid fraction (c).

3 RESULTS AND DISCUSSION

3.1 Chemical composition analysis of the samples

The final composition of steel and slag samples (after the melting experiment) is shown in Table 3 and 4, respectively.

Table 3. Final steel composition, wt.%.

Sample	C	Si	Mn	P	Cr	Ni	Mo	Al_t	S*	T.O.*	N*
1	0.90	0.88	0.823	0.026	0.155	0.03	0.01	0.016	14	16.5	79
2	0.67	0.49	0.843	0.020	0.157	0.03	0.01	0.030	10	23.5	98
3	0.94	0.95	0.812	0.026	0.155	0.03	0.01	0.023	13	20	80
4	0.63	0.55	0.841	0.015	0.162	0.03	0.01	0.030	10	11.5	75

**ppm*

Table 4. Final slag composition, wt.%.

Sample	CaO	SiO_2	Al_2O_3	MgO	wt.% CaO/ wt.% SiO_2	wt.% CaO/ wt.% Al_2O_3
1	43.28	25.19	9.79	21.45	1.72	4.42
2	52.77	19.20	10.37	17.46	2.75	5.09
3	39.56	18.69	18.98	22.47	2.12	2.08
4	47.63	18.03	20.89	13.26	2.64	2.28

It is noted some differences in C, Si, Al, S, T.O. and N contents, compared to the initial steel composition, as seen in Table 3. The increase in C and Si is possibly related to the reaction with the refractory material. The Al also increased for almost all steel samples. On the other hand, as expected, S, T.O. and N decreased after the experiment, resulting from the refining reactions between slag and steel. The lowest and highest values of T.O. were observed for samples 4 and 2, respectively. Unexpectedly, it is observed that the T.O. was not affected by the increase of the slag basicity. In fact, the steel sample 2 presented practically the same content of the T.O. and the smallest change of N, compared to the initial sample. This may be a consequence of the presence of small internal defects in this sample after melting process, making the value still high during the analysis of T.O. and N contents. Even so, the decrease in N in the samples is clear and this can be attributed to the use of a protective atmosphere during the experiment, disfavoring air reoxidation [5], but also to the degassing effect, since the nitrogen content in the flowing gas is low (< 3 ppm), favoring a new equilibrium condition, between the atmosphere nitrogen and the nitrogen from steel, promoting the decrease in the nitrogen content in the steel (which is higher, as shown in Table 3).

Regarding the composition of slags, Table 4 shows that the MgO content in the slags increased after all experiments compared to the initial composition. This effect is attributed to the reaction involving the slag and the refractory material of the crucible (MgO-C). In this context, it is important to observe the adjustment of the slag composition to attain MgO saturation. Figure 2 shows slags from samples 1 to 4 and their solid fraction evolution with increasing MgO predicted by *FactSage*™ 7.2 at 1600 ºC.

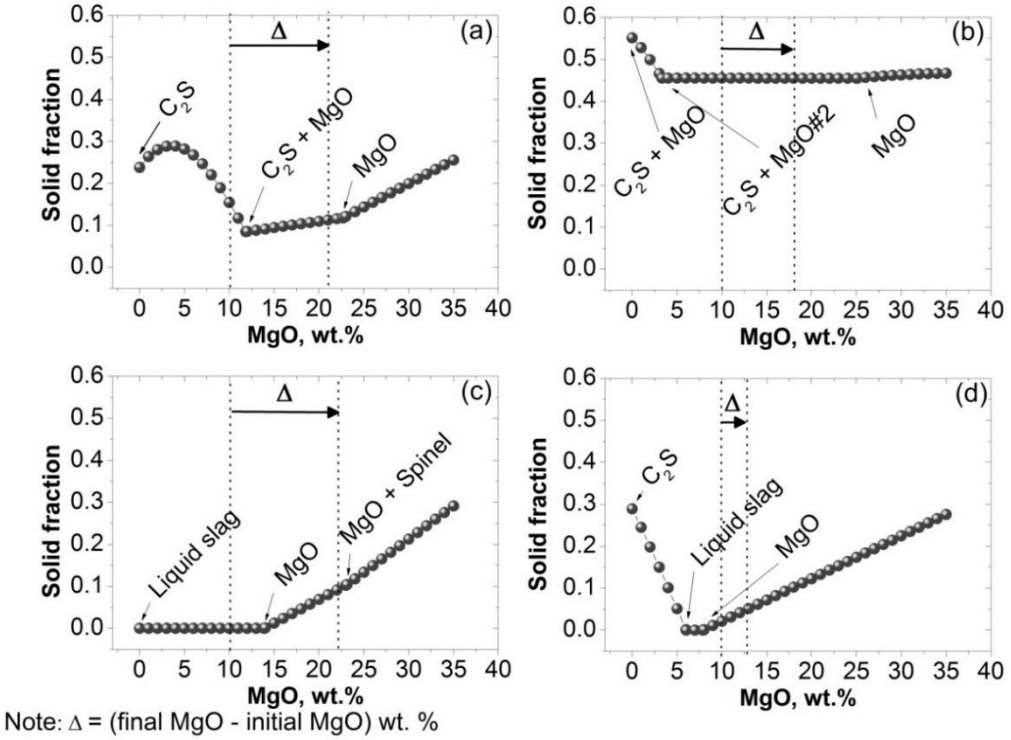

Figure 2. Solid fraction of slags as a function of MgO content at 1600 ºC for slags (a) 1, (b) 2, (c) 3 and (d) 4. Predicted by *FactSage*™ 7.2.

By Figure 2 it is possible to identify the beginning of the saturation process in the slag, through the analysis of the phases that are formed. The saturation condition in MgO is identified in the region where there is precipitation of MgO solids. The exact values of MgO saturation calculated by *FactSage*™ for slags 1, 2, 3 and 4 are, respectively, 11.8, 3.3, 13.9, 7.9 wt.%. The MgO saturation content is affected by the binary basicity of the slag. When the binary basicity is lower, more MgO is required in the slag to reach the saturation condition (as represented by Figure 2 and Table 4).

In the case of slags from samples 1 (Figure 2a) and 2 (Figure 2b), this precipitation occurs initially along with the C_2S phase. Only around 25 wt.% there is single precipitation of the MgO phase. On the other hand, the slags from samples 3 (Figure 2c) and 4 (Figure 2d) do not present the combined precipitation of C_2S with MgO. However, these slags present formation of liquid slag for a specific range of MgO. Immediately to the formation of liquid slag, there is then saturation in MgO.

The difference between the MgO content in the slag before and after the experiments (Δ) can be interpreted as an index of the corrosion degree of refractory from crucible [7]. Figure 2d shows that the slag from sample 4 is the only one within the region where there is only MgO precipitation and, for that reason, being the one with the lowest variation of the MgO content in the slag. However, Figure 2c shows the largest variation, possibly because it was in a totally liquid condition for 1600 ºC.

Figure 3 shows an important relation of the chemical composition of the slag with respect to the removal of S from the steel.

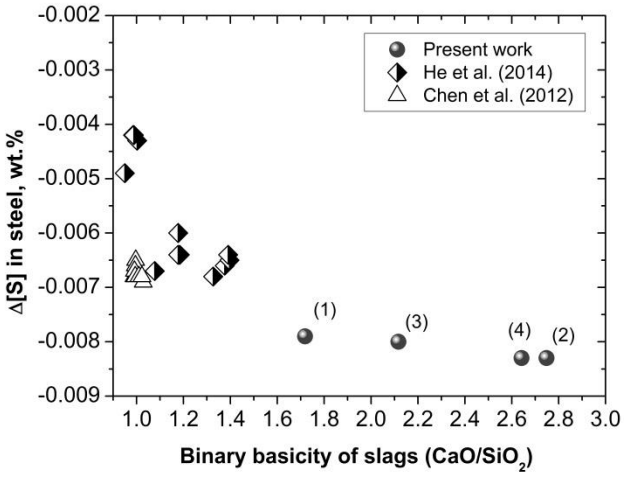

Figure 3. Effect of the binary basicity of slags in the S removal from steel.

Knowing that desulphurization is favored by the increase of slag basicity [8,9], Figure 3 shows a very satisfactory result. Indirectly, it can be inferred that there was a good interaction between slag and steel during the experiment, considering that the S removal is favored by the reactions involving slag and liquid steel. This fact is also very relevant for the removal of inclusions by slag.
With respect to the Al_2O_3 content in the slag, it is possible to identify an effect on Al in the steel, as shown in Figure 4.

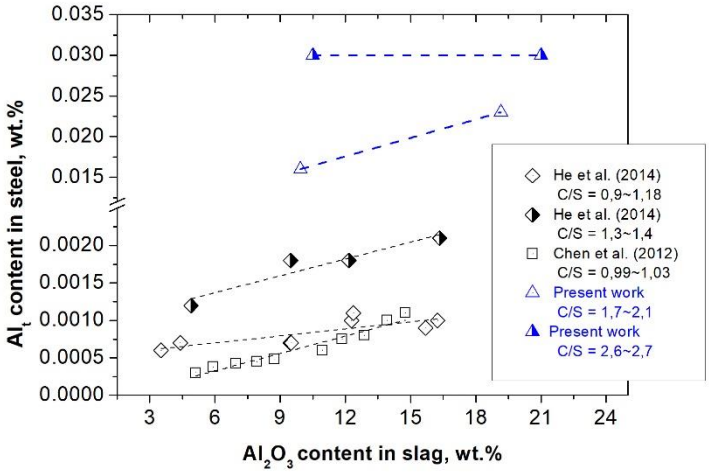

Figure 4. Effect of Al_2O_3 in slag in the Al content in steel.

According to Chen *et al*. [8], the Al content in the steel is controlled by the steel/slag reactions. In view of that, Figure 4 shows that as the Al_2O_3 content is raised in the slag, the Al content in the steel tends to increase as well. It is also observed that the increase of the binary basicity of the slag affects the amount of Al in the steel, promoting a higher Al as the basicity increases. This effect is quite clear when basicity is increased in the range of 1.7-2.1 to 2.6-2.7 and the Al_2O_3 content in the slag is kept fixed. All these effects are in agreement with previous studies [8,9]. However, for the greater range of binary basicity (2.6-2.7), the increase of Al with the increase of Al_2O_3 was not observed, since the Al content remained constant at 0.030 wt.%.

3.2 Liquid fraction and viscosity of slags

In the equilibrium, the composition of the liquid fraction of slags plays an important role, considering that this fraction effectively participates in the refining reactions involving the slag and steel and, specially, the removal of inclusions. Thus, it is important to establish the amount of liquid present in the slag and the chemical composition for a given temperature. Table 5 presents some information about the liquid fraction of slags, obtained through computational thermodynamics and based on the initial and final composition of the slags used for the experiment at 1600 ºC.

Table 5. Slags fractions and chemical composition of the liquid (wt. %) and its viscosities (Pa.s) at 1600 ºC. Predicted by *FactSage*™ 7.2.

Sample	Fraction		Chemical composition of liquid fraction (wt.%)						Viscosity (Pa.s)	
	Liquid	Solid	CaO	SiO_2	Al_2O_3	MgO	wt.% CaO/ wt.% SiO_2	wt.% CaO/ wt.% Al_2O_3	Liquid	Solid + Liquid
1 (Initial)	0.84	0.16	45.48	31.40	11.83	11.29	1.45	3.85	0.104	0.158
1 (Final)	0.71	0.29	47.49	27.85	13.82	10.84	1.71	3.44	0.096	0.227
2 (Initial)	0.54	0.46	58.11	18.56	18.31	5.02	3.13	3.17	0.077	0.351
2 (Final)	0.57	0.43	58.11	18.56	18.31	5.02	3.13	3.17	0.077	0.320
3 (Initial)	1.00	0.00	42.00	28.00	20.00	10.00	1.50	2.10	0.130	0.130
3 (Final)	0.86	0.14	45.99	21.74	22.03	10.24	2.12	2.09	0.104	0.151
4 (Initial)	0.98	0.02	51.11	20.45	20.44	7.99	2.50	2.50	0.092	0.097
4 (Final)	0.94	0.06	50.60	19.16	22.19	8.05	2.64	2.28	0.093	0.108

From Table 5, it can be observed that in relation to the composition of the liquid part of the slag there was no significant variations, comparing the initial condition with the final (after experiment). However, there are some variations in the liquid and solid fraction of slag, resulted, naturally, by the reactions that occurred at 1600 ºC, involving the crucible/slag/steel system. After experiment condition, it is possible to notice that the slags from Table 5 presented variable liquid fractions, ranging from 0.57 to 0.94. As expected, as the liquid fraction increases, the effective viscosity (solid + liquid) decreases. Additionally, it is observed that the larger the solid fraction of the slag, the greater the difference between viscosity and effective viscosity. This fact is evidenced by slag 2, with a high solid fraction (0.43) the difference between the viscosities is 0.243 Pa.s. Reis, Bielefeldt and Vilela [10] reported this same observation.

The lowest effective viscosity is obtained by slag 4, with 0.108 Pa.s. In contrast, the slag 2 shows the higher viscosity, in consonance with its high solid fraction. It is noted that the solid and liquid fraction of a given slag has an explicit influence on its viscosity and variations in the chemical composition of the slag is capable of producing different distributions of these phases.

3.3 Inclusion analysis

The inclusion analysis of the steel samples after experiments highlights the role of slag in the removal of inclusions from liquid steel, through the reactions in the slag/steel interface. The refining potential of the slags studied can be presented from the point of view of the changes identified in inclusions density per steel sample, as illustrated by Figure 5(a). The results for the density change of the inclusions were

achieved by taking the difference between the inclusion density after and before experiment. Another important result is with regard to the evolution of the composition of all inclusions detected, as shown in Figure 5(b).

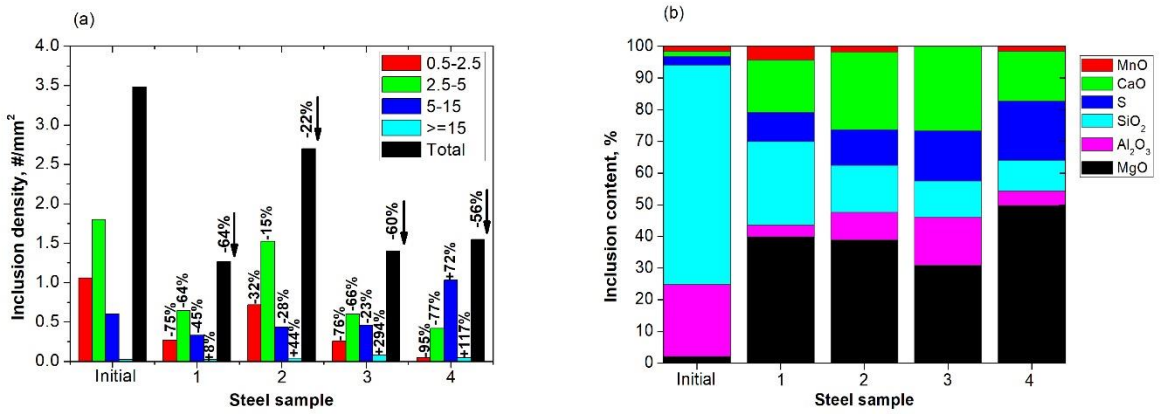

Figure 5. (a) Inclusion density change and (b) average chemical composition of inclusions per steel sample.

In general, in all cases shown by the Figure 5(a), there is a clear decrease in the inclusions density. The largest change occurs for the experiment in sample 4, with an approximate drop of -95% particularly in the size range of 2.5-5 μm. Although an increase in the density of larger inclusions (≥ 15 μm) was observed by using the slags, these values are considered very low, being less than 0.08 inclusions/mm^2. This increase is due to the incorporation of Mg in the inclusions and also probably by entrapment of slag particles (or refractory material). This effect was favored by the slag of lower viscosity and solely saturated in MgO (Figure 2(d)). The result can be observed by the Figure 5(b), showing that for the slag 4 the inclusions formed have the highest content of MgO. Considering the absolute change in the inclusion population, a decrease of at least 56% is observed using slags 1, 3 and 4.

Figure 5(b) shows that the inclusions of the initial sample of steel were basically of the system Al_2O_3-SiO_2 which, after the reactions with the slag, evolved to inclusions richer in MgO, with lower contents of Al_2O_3 and SiO_2.

Through another approach, the density of inclusions presents a reasonable relationship with the T.O. content in the steel, as shown in Figure 6.

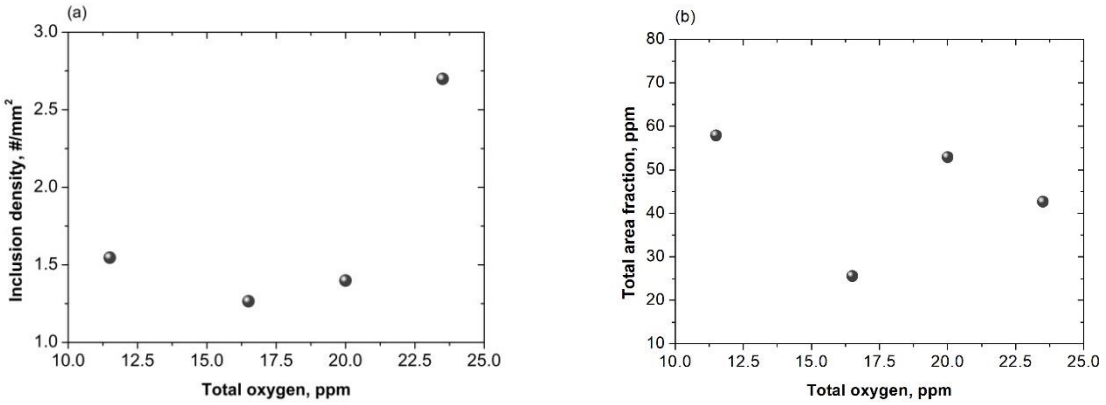

Figure 6. Relation of T.O. with the (a) inclusion density and (b) total area fraction of inclusions.

The T.O. content takes into account the sum of dissolved oxygen and the oxygen in oxides (inclusions). According to Zhang [11], the value of T.O. can be used as an

indirect measure of the content of inclusions present in the steel. In fact, Figure 6(a) identifies a reasonable relation of the inclusions density as a function of the T.O. content in steel. As expected, as the T.O. increases, the inclusion population in steel tends to be larger. However, no clear relationship was obtained with the total area fraction of inclusions, as shown by Figure 6(b). In this way, it can be inferred that the oxygen content dissolved in the steel samples may affected the results of T.O., since even for low T.O. contents, high area fraction indexes were obtained.

3.3 Slags and their relation with steel cleanliness

Figure 7 shows the influence of the effective viscosity of the slag in the steel cleanliness, through the inclusion removal efficiency and in the T.O. content.

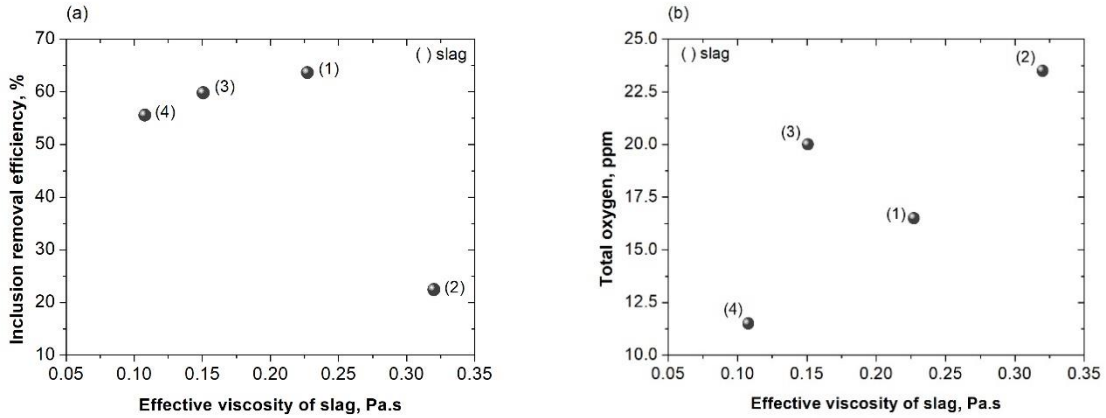

Figure 7. (a) Effect of the effective viscosity of slags in the inclusion removal and (b) in the T.O. content.

Figure 7(a) shows that slags 1, 3 and 4 showed the best results from the point of view of the efficiency to remove inclusions from the liquid steel, with removal efficiency above 55%. However, the slag 2 proved to be worse in the inclusion removal with approximately 22% efficiency. Based on Figure 7(a), the removal of inclusions shows a tendency to improve, as the slag viscosity decreases (< 0.23 Pa.s). In comparison with the other slags, slag 2 presented the highest solid fraction and, therefore, higher effective viscosity. This result contributed to the low effectiveness in steel cleanliness, considering that the interaction between slag and steel is weakened with the use of high viscosity slags. For improving the efficiency in the removal of inclusions, the design of slags with the lowest effective viscosities should be sought [10].

From another perspective, by Figure 7(b), it also can be observed that slags with lower viscosities tend to produce steels with lower T.O. content. This effect is closely related to the reduction of the inclusion density in steel, since there is a relation of T.O. with the population of inclusions, as shown previously (Figure 6).

Although possessing better inclusions removal capacity, slags with lower viscosities, promote increase in the area fraction of Mg rich inclusions in the experiment (Figure 8).

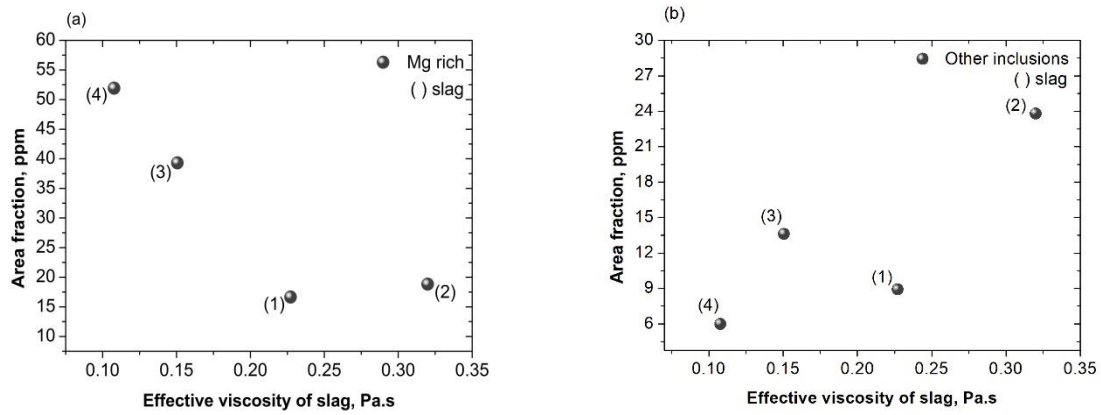

Figure 8. Effective viscosity of slag effect in the area fraction of (a) Mg rich inclusions and (b) other type (remained) inclusions.

The effect shown in Figure 8(a) can be related to the interaction degree of the slag both as steel but also with the refractory material of the crucible. Thus, slags with lower viscosity tend to attack the refractory, promoting the incorporation of Mg rich particles in the form of inclusions [12]. According to Li *et al*. [12], the corrosion of the refractory material is not only a function of the MgO solubility, but also of the slag viscosity. On the other hand, Figure 8(b) shows that, in fact, slags with lower viscosity present better cleanliness conditions to the liquid steel, considering the smallest area fraction of others inclusions identified.

Figure 9 shows the distribution of the inclusions with a minimum size of 2.5 μm identified for each steel sample, through the CaO-Al_2O_3-MgO system.

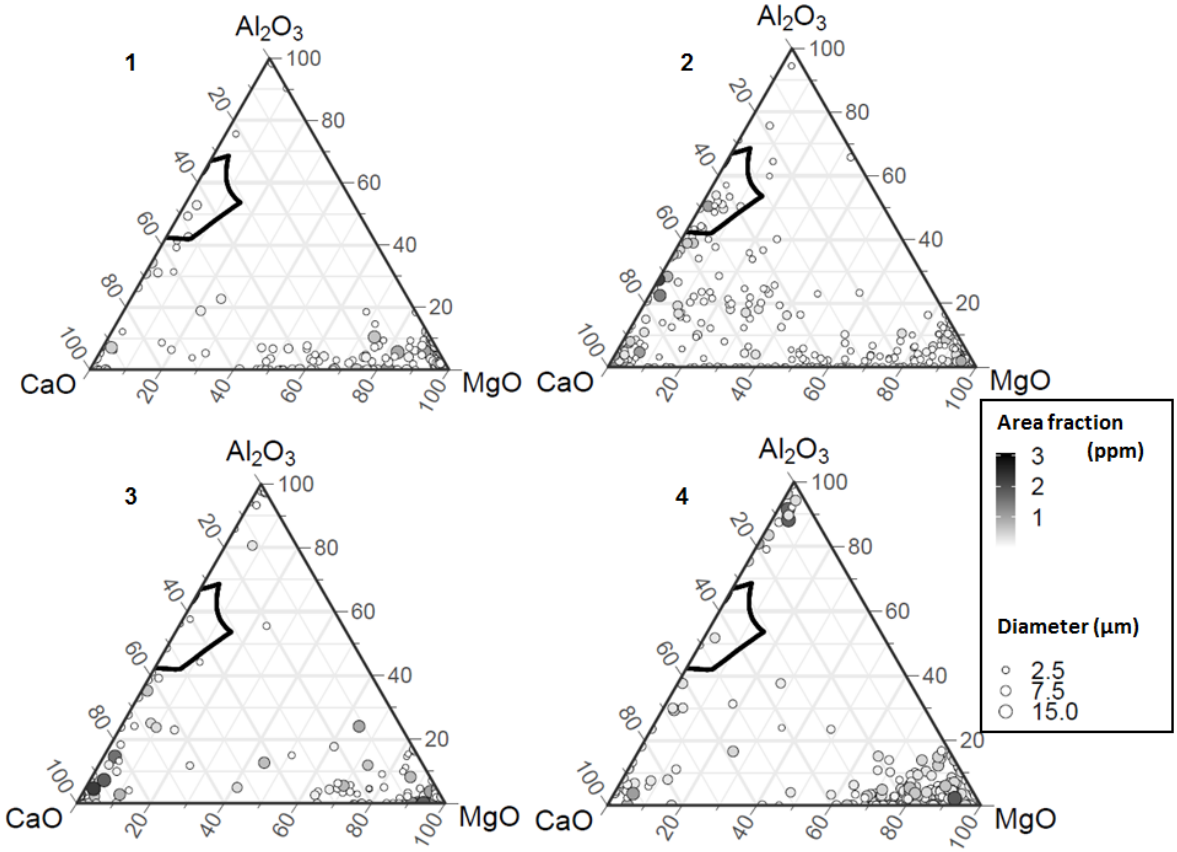

Figure 9. Inclusion distribution in the CaO-Al_2O_3-MgO system (mass %) with 1600 ºC for each steel sample.

In all cases shown by Figure 9, it is observed that there are many inclusions in the MgO region, corroborating to the reactions occurred in the refractory/slag/steel system. Additionally, it is noted that are present some inclusions with high CaO content, and this effect can be related to the wt.% CaO/wt.% SiO_2 ratio in the liquid slag, that promotes an increase in the area fraction for CaO-based inclusions. This behavior may be related to the interaction of the initial sample containing Si and Al based inclusions with the high basicity liquid slag during the experiment, occurring the incorporation of Ca in the modification of inclusions and, consequently, increasing its area fraction. Still analyzing Figure 9, sample 2 presents the most heterogeneous distribution in terms of inclusion. Additionally, there are still some inclusions in the Al_2O_3 region for sample 4 and few others in sample 3. This behavior is in agreement with the greater supply of Al_2O_3 in the slag (Tables 4 and 5), which even more fluid, may have caused the incorporation of particles rich in Al_2O_3 by emulsification.
With respect to the reaction involving slag and crucible material, the reaction promotes the dissolution of the MgO of the crucible, which can therefore react with the metal and be reduced through Al to form Mg (Figure 10).

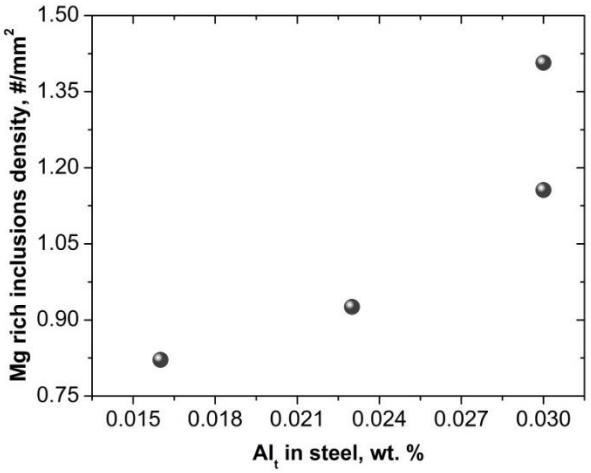

Figure 10. Effect of MgO reduction by Al from steel in the formation of inclusions rich in Mg.

The Mg continues to react and form inclusions of the MgO/MgS type, according to the reactions 3 and 4. Additionally, low viscosity and already saturated slags in MgO can also interact with the liquid metal and promote the reactions, resulting in the incorporation of inclusions rich in Mg.

$$MgO_{(slag)} + Al_{(steel)} \rightarrow Al_2O_{3(inclusion)} + Mg_{(steel)} \quad (3)$$

$$Mg_{(steel)} + O/S_{(steel)} \rightarrow MgO/MgS_{(inclusion)} \quad (4)$$

Figure 10 shows the reduction of the MgO by the Al in the steel, promoting an increase of the inclusion density rich in Mg. The increase of the Al content in the steel is triggered by the use of slags with higher contents of Al_2O_3, previously shown by Figure 4. Consequently, there is a greater supply of Al to reduce MgO.

4 CONCLUSIONS

The present experimental and thermodynamic study applied for CaO-SiO_2-Al_2O_3-MgO slag systems allowed to identify that changes in their composition presented effects on the steel cleanliness. In general, the total inclusion density decreased (at least 22%) by using CaO-SiO_2-Al_2O_3-MgO slags. The slags from samples 1, 3 and 4 presented a small difference in the efficiency of removal of inclusions, being between 56 to 64%. Therefore, all these slags can be considered potential for inclusionary cleanliness, following the sequence of higher capacity: slag 1 > slag 3 > slag 4 > slag 2. The lowest T.O. content (11.5 ppm) was obtained with the use of slag 4, although the slag 4 generated inclusions with higher content of MgO. As expected, the removal of inclusions by slags shows a tendency to improve as their viscosity decreases (< 0.23 Pa.s). However, lower viscosity slags (< 0.15 Pa.s) presented a greater tendency to promote the formation of inclusions rich in Mg with larger area fraction, due to the better interaction between slag (rich in MgO) with steel and also with the crucible material.

Acknowledgments

We thank the CNPq, CAPES and Luiz Englert Foundation for financial supports.

REFERENCES

1 Ban-Ya S. Preface. ISIJ International. 1993; 33(1):1.
2 Jiang M, Wang XH, Wang WJ. Study on refining slags targeting high cleanliness and lower melting temperature inclusions in Al-killed steel. Ironmaking and Steelmaking. 2012; 39(1):20-25.
3 Strandh J, Nakajima K, Eriksson E, Jönsson P. Solid inclusions transfer at a steel–slag interface with focus on tundish conditions. ISIJ International. 2005; 45(11):1597–606.
4 Rocha VC, Alves PC, Pereira JAM, Leal LP, Bielefeldt WV, Vilela ACF. Experimental and thermodynamic analysis of MgO saturation in the CaO–SiO_2–Al_2O_3–MgO slag system melted in a laboratory resistive furnace. Journal of Materials Research and Technology. 2018; 8(1):861-870.
5 Alves PC, Pereira JAM, Rocha VC, Bielefeldt WV, Vilela ACF. Laboratorial Analysis of Inclusions Formed by Reoxidation in Tundish Steelmaking. Steel Research International. 2018; 89(11):1-11.
6 Roscoe R. The viscosity of suspensions of rigid spheres; British Journal of Applied Physics. 1952; 3:267-269.
7 Ren Y, Zhang L, Fang W, Shao S, Yang J, Mao W. Effect of Slag Composition on Inclusions in Si-Deoxidized 18Cr-8Ni Stainless Steels. Metallurgical and Materials Transactions B. 2016; 47(2):1024-1034.
8 Chen S, Jiang M, He X, Wang X. Top slag refining for inclusion composition transform control in tire cord steel. International Journal of Minerals, Metallurgy, and Materials. 2012; 19(6):490-498.
9 He XF, Wang XH, Chen SH, Jiang M, Huang FX, Wang WJ. Inclusion composition control in tyre cord steel by top slag refining. Ironmaking and Steelmaking. 2014; 41(9): 676-684.
10 Reis BH, Bielefeldt WV, Vilela ACF. Efficiency of inclusion absorption by slags during secondary refining of steel. ISIJ International. 2014; 54(7):1584-1591.
11 Zhang L. Indirect methods of detecting and evaluating inclusions in steel. Journal of Iron and Steel Research. 2006; 13(4):1-8.
12 Li X, Wang L, Yang S, Zhuang C. Effect of slag composition on the cleanliness of drill rod steel. Ironmaking and Steelmaking. 2019; 46(5):416-423.